

Two-Photon Dyes Containing Heterocyclic Rings with Enhanced Photostability

Hwan Myung Kim,^[a] Wen Jun Yang,^[b] Chang Ho Kim,^[a] Won-Hwa Park,^[a] Seung-Joon Jeon,^{*,[a]} and Bong Rae Cho^{*,[a]}

Abstract: A series of donor- π -donor derivatives containing phenyl, naphthyl, and anthryl groups as the π -center and heterocyclic rings as the conjugation bridge have been synthesized and their one- and two-photon spectroscopic properties and photostability were

determined. These compounds show bathochromic shifts in the absorption

Keywords: dyes • fluorescence • heterocycles • two-photon absorption • vesicles

and emission spectra, larger two-photon cross-section, and enhanced photostability in comparison to their open-chain analogues. In addition, a convenient method for the qualitative photostability measurement is proposed.

Introduction

Recently, two-photon microscopy (TPM) has become a vital tool for live-tissue imaging.^[1] The advantages of TPM are improved penetration depth, localized two-photon (TP) excitation, reduced photodamage and photobleaching, small absorption coefficient of light in tissue, and lower tissue auto-fluorescence.^[2] For maximum utilization of TPM, it is crucial to develop efficient two-photon probes for specific applications. A useful probe for such applications should have i) a large TP cross-section (δ_{TPA}) in the NIR-IR region, ii) appreciable solubility in water, iii) high photostability, and

iv) receptors for the biological substrates. Recent work has shown that TP dyes with δ_{TPA} values exceeding 5000 GM can be synthesized by optimizing the molecular structures.^[3] Also, water soluble TP dyes with significant δ_{TPA} have been reported.^[4] Furthermore, TP probes sensitive to the metal ions and pH have been developed.^[5,6] However, except for a few studies on the photostability of the TP dyes in solution, virtually nothing is known about it under imaging conditions.^[7]

The most actively investigated structural motifs for TP materials are donor-bridge-donor (D- π -D) quadrupoles, in which the donors are connected to the π center via C=C bonds.^[3,8] However, this bond readily undergoes *trans* to *cis*-photoisomerization, which may hamper the efficiency and the lifetime of the materials.^[8b,9] This problem can be avoided if one incorporates the double bond within a ring. For this purpose, we have synthesized a series of D- π -D derivatives containing phenyl, naphthyl, and anthryl groups as the π center and heterocyclic rings as the conjugation bridge (Scheme 1). We have determined one- and two-photon spectroscopic properties, two-photon cross-sections, and photostabilities of **1–4**. We now report that these compounds show large δ_{TPA} in solutions and enhanced photostability in giant unilamellar vesicles (GUVs).

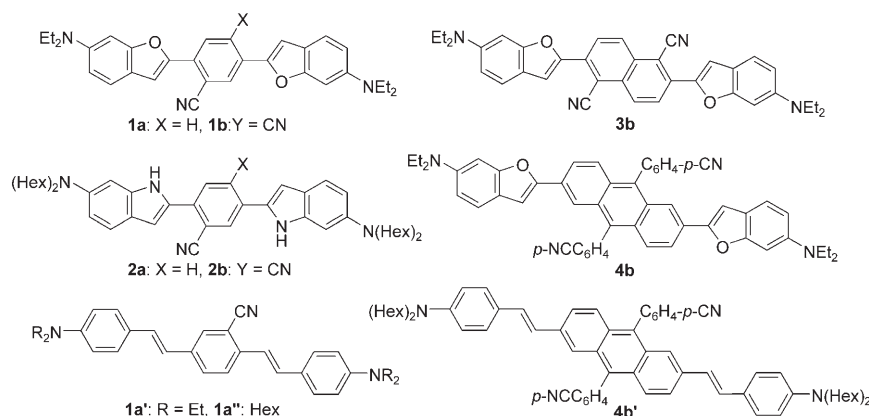
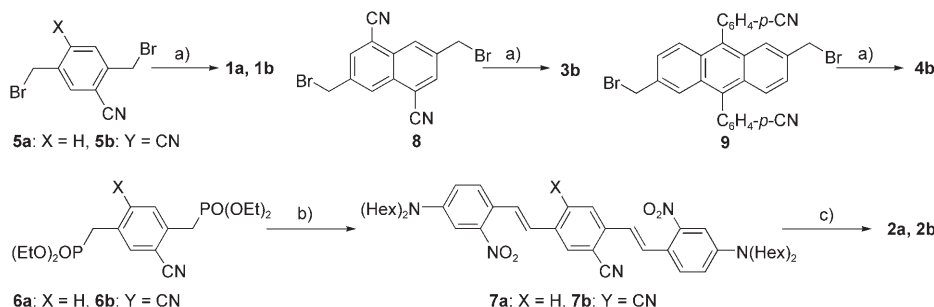
Results and Discussion

Synthesis: Synthesis of **1–4** is shown in Scheme 2. Reactions of **5a** and **5b** with 4-(diethylamino)salicylaldehyde produced **1a** and **1b** in 42–48% yields. Compounds **3b** and **4b** were

[a] H. M. Kim, Dr. C. H. Kim, W.-H. Park, Prof. S.-J. Jeon, Prof. B. R. Cho
Molecular Opto-Electronics Laboratory
Department of Chemistry and Center for Electro- and Photo-Responsive Molecules
Korea University, 1-Anamdong
Seoul 136-701 (Korea)
Fax: (+82)2-3290-3121
E-mail: chobr@korea.ac.kr

[b] Prof. W. J. Yang
Key Lab of Rubber-Plastics
Ministry of Education
(Qingdao University of Science and Technology)
53-Zhengzhou Road
Qingdao 266042 (China)

Supporting information for this article is available on the WWW under <http://www.chemeurj.org/> or from the author: Fluorescence spectra of GUVs stained with **1–3** in buffer solution pH 7.0, TPEF images of equatorial sections of GUVs labeled with **1a** and **1a'**, decay rates of TPEF in small GUVs labeled with **1–3**.

Scheme 1. Structures of D- π -D derivatives used in this study.Scheme 2. a) 4-(Diethylamino)salicylaldehyde, Bu_4NHSO_4 , K_2CO_3 , DMF, 125°C , 8 h; b) $\text{NaO}t\text{Bu}$, THF, 4-(di-hexylamino)-2-nitrobenzaldehyde, $0-25^\circ\text{C}$, 12 h; c) $\text{P}(\text{OEt})_3$, 160°C , 12 h.

synthesized in 34–61 % yields by the same procedure as described for **1a**.

To synthesize **2a** and **2b**, **6a** and **6b** were treated with 4-(dihexylamino)-2-nitrobenzaldehyde to obtain **7a** and **7b** in 78–84 % yields. The latter were then reacted with $\text{P}(\text{OEt})_3$ to produce **2a** and **2b** in 24–37 % yields. The structures of **1–4** were unambiguously characterized by ^1H NMR, IR spectroscopy, and elemental analysis.

One-photon absorption and emission spectra: Figure 1 shows the absorption and emission spectra of **1–4**. The spectral properties of **1–4** are compared with the corresponding open-chain analogues in Table 1. As expected, both $\lambda_{\text{max}}^{(1)}$ and $\lambda_{\text{max}}^{\text{fl}}$ increase gradually with a stronger acceptor, that is, **1a** < **1b**, **2a** < **2b**. On the other hand, the values are almost the same for **1b** and **3b**, despite extended conjugation. Furthermore, $\lambda_{\text{max}}^{(1)}$ and $\lambda_{\text{max}}^{\text{fl}}$ of **1a**, **1b**, and **4b** are significantly red-shifted in comparison to the open-chain analogues. This finding suggests that the intramolecular charge transfer (ICT) is significantly enhanced by the increased planarity and the presence of the additional heteroatom donors in the heterocyclic rings. Except for **2b**, all of the compounds show modest to high quantum yields. Interestingly, the fluorescence lifetimes are longer for the heterocyclic compounds than for the open-chain analogues, although they are almost the same in toluene and in GUVs (Table 1).

Two-photon cross-sections: The two-photon cross-sections (δ_{TPA}) of **1–4** were measured by using femtosecond laser pulses as described.^[3] The two-photon excitation spectra for **1–4** are depicted in Figure 2. Table 1 summarizes the relevant spectroscopic parameters. Most compounds exhibit broad TP absorption bands in the 740–1000 nm spectral regions, which is useful for application to TPM. In addition, an additional CN group in **1b** and **2b** results in a two-fold increase in the δ_{max} values of **1a** and **2a**. Except for **1b** and **1b'**, δ_{max} values are always larger for the heterocyclic compounds than for the open-chain analogues. Also, there is a qualitatively linear relationship between δ_{max} and $\lambda_{\text{max}}^{(1)}$ (Table 1). Furthermore, the δ_{max} value of **2b** is larger than **3b** and **4b** has the largest value. The parallel increase in the δ_{max} with ICT and molecular size is well documented in the literature.^[3,7] Finally, **1a** shows significant $\delta_{\text{max}} = 510 \text{ GM}$ in

EtOH at 800 nm, which makes it an attractive two-photon fluorophore for bio-imaging.

Photostability: The photostability was determined by using TPM ($\lambda = 800 \text{ nm}$, $I = \sim 1.2 \text{ mW } \mu\text{m}^{-2}$) on GUVs grown from mixtures of 1,2-dipalmitoyl-*sn*-glycero-3-phosphocholin (DPPC) phospholipid and **1–3**. GUVs with mean diameters of $\sim 10 \mu\text{m}$ (**1–3**) and $\sim 100 \mu\text{m}$ (**1a'**, **2a**) were obtained by solvent evaporation and electroformation methods, respectively.^[10] We could not measure the photostability of **2b**, **4b**, and **4b'** because TPEF of **2b** was too weak to be detected accurately and DPPC GUVs did not grow when stained with **4b** and **4b'**.

As shown in Figure 3, the dyes stain the membranes and appear to be parallel to the membrane lipids.^[11] In addition, $\lambda_{\text{max}}^{\text{fl}}$ of **1a'** and **2a** in GUVs are nearly identical to those in toluene, indicating that the dyes may be buried deeply inside the membrane (Table 1). This outcome could result because these compounds have $(\text{Hex})_2\text{N}$ rather than Et_2N as the donor, providing better interactions with the hydrophobic tails. On the other hand, $\lambda_{\text{max}}^{\text{fl}}$ of **1a** in GUVs is between those measured in toluene and EtOH. Also, $\lambda_{\text{max}}^{\text{fl}}$ of **1a'**, **1b**, **1b'**, and **3b** are significantly more red-shifted in GUVs than in toluene (Figure S1 in the Supporting Information). This result indicates that these dyes are located more toward the

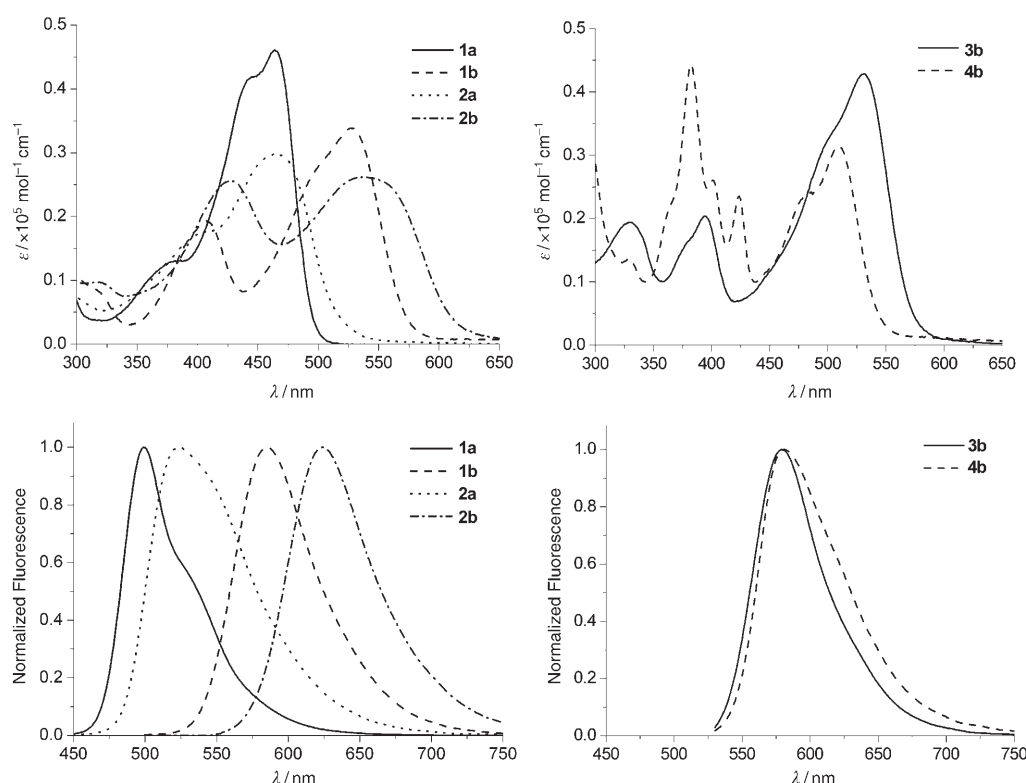


Figure 1. Molar absorptivity and normalized emission spectra of **1–4** in toluene.

Table 1. Photophysical Data for **1–4**.^[a]

Cpd	$\lambda_{\text{max}}^{\text{[b]}}$	$\lambda_{\text{max}}^{\text{fl [c,d]}}$	$\Phi^{\text{[e]}}$	$\tau^{\text{[f,g]}}$	$\lambda_{\text{max}}^{(2) \text{ [h]}}$	$\delta_{\text{max}}^{\text{[i]}}$	$t_{1/2}^{\text{[j,k]}}$
1a	464	498 (525)	0.95	1.63 (1.63)	780	700	280
1a ^[l]	459	541	0.61	2.42	800	510	
1a ^[m]	426	483 (500)	0.52	0.65 (0.72)	740	260	100
1a ^[n]		(480)		(0.72)			(410)
1b	527	584 (604)	0.41	2.92	880	1510	200
1b ^[n]	490	536 (583)	0.69	1.39	830	1750	110
2a	463	520 (518)	0.52	2.14 (1.90)	800	690	240 (720)
2b	538	624	0.07	2.19	900	1810	
3b	532	579 (627)	0.42	2.44	900	1370	180
4b	509	581	0.38	2.52	880	2150	
4b ^[o]	488	535	0.64	2.39	840	1570	

[a] Solvent was toluene except where otherwise noted. [b], [c] λ_{max} of the one-photon absorption and emission spectra in nm. [d], [g] The numbers in the parentheses are $\lambda_{\text{max}}^{\text{fl}}$ and τ of the small GUVs, respectively. [e] Fluorescence quantum yield. [f] Fluorescence lifetime in nanoseconds. [h] λ_{max} of the two-photon excitation spectra in nm. [i] The peak two-photon absorptivity in $10^{-50} \text{ cm}^4 \text{ s per photon (GM)}$. [j] Two-photon excited fluorescence (TPEF) decay half-life ($t_{1/2}$) of small GUVs. [k] The numbers in the parentheses are $t_{1/2}$ of large GUVs. [l] Solvent was EtOH. [m] Ref. [8b]. [n] Ref. [8a]. [o] Ref. [8e].

hydrophilic-hydrophobic interface than are **1a**^[n] and **2a** in the membranes.

The TPEF intensity from the dyes in the large GUVs decreased gradually with irradiation time under the TPM. As expected, the photobleaching rate is first-order to the substrate, with half-lives of 410 and 720 s for **1a**^[n] and **2a**, respectively (Figure 3).^[12] This observation indicates that incorporating the C=C bond within a ring enhances the photostability by a factor of two. The photostability of the small GUVs was determined by the same method, except that the

laser beam was focused more tightly ($I = \sim 120 \text{ mW } \mu\text{m}^{-2}$). Table 1 shows that $t_{1/2}$ of the heterocyclic compounds and open-chain analogues in the small GUVs are in the range of 180–280 and 100–110 s, respectively. Here again, a two-fold enhancement is evident in the former, even though $t_{1/2}$ is significantly shorter. Note that $t_{1/2}$ of **2a** is three times shorter in small GUVs than in larger ones, although they are expected to be located in almost the same region of the membranes. Thus, the much smaller $t_{1/2}$ in small GUVs can be attributed to the more tightly focused

laser beam, not to the change in the environment. It was previously reported that the primary causes of photochemical instability of one- or two-photon dyes are the photooxidation and photoisomerization of the C=C bond.^[7,8b,9,12] Because the oxygen concentration in the GUVs should be almost the same, the enhanced photostability of the heterocyclic compounds observed in this study can be attributed to the inhibition of the latter.

Finally, we propose that this approach is a useful method for a qualitative photostability test. Growing the small

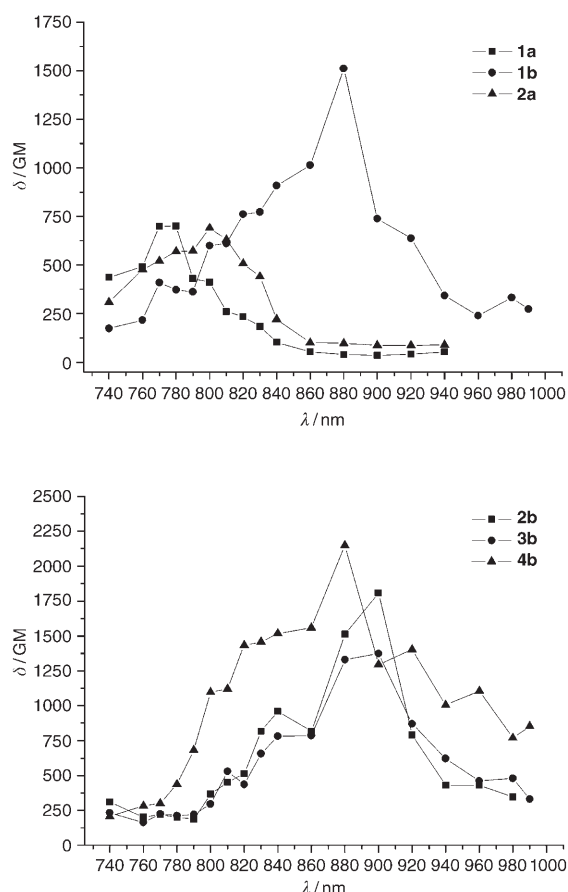


Figure 2. Two-photon excitation spectra for **1–4** in toluene.

GUVs is relatively easy and TPM experiments can be carried out using the same set-up for the bio-imaging. In addition, GUVs are a good model for biological membranes.

Conclusion

In this paper, the photophysical properties and photostability of a series of D- π -D derivatives containing heterocyclic rings in the conjugation bridge have been investigated. Overall, these compounds show larger values of $\lambda_{\max}^{\text{fl}}$, $\lambda_{\max}^{(2)}$, δ_{\max} and enhanced photostability in comparison to the open-chain analogues. Furthermore, a convenient method for the photostability test for TP materials is proposed. This result underlines the usefulness of the heterocyclic ring as the conjugation bridge for the efficient two-photon probes for TPM applications.

Experimental Section

Synthesis: 2-Cyano-1,4-bis(*p*-diethylaminostyryl)benzene (**1a'**), 2-cyano-1,4-bis(*p*-dihexylaminostyryl)benzene (**1a''**), 2,5-dicyano-1,4-bis(*p*-diethylaminostyryl)benzene (**1b'**), 9,10-bis(*p*-cyanophenyl)-2,6-bis(*p*-dihexylaminostyryl)benzene (**4a'**) were either available from previous study or syn-

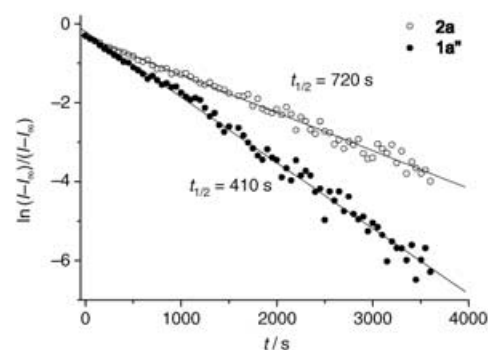
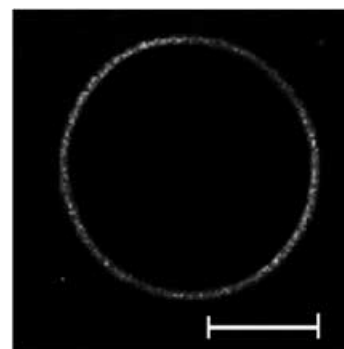


Figure 3. Top: TPEF image of the GUV labeled with **2a**. The excitation light ($\lambda = 800$ nm, $I = \sim 1.2$ mW μm^{-2}) is polarized parallel to the horizontal axis of the image. The scale bar equals 100 μm . Bottom: Decay rates of the TPEF in GUVs labeled with **2a** and **1a''**.

thesized as reported.^[5b,8a,8b,8e] 1,4-Bis(bromomethyl)-2-cyanobenzene (**5a**), 1,4-bis(bromomethyl)-2,5-dicyanobenzene (**5b**), 1,4-bis[(diethoxyphosphoryl)methyl]-2-cyanobenzene (**6a**), 1,4-bis[(diethoxyphosphoryl)methyl]-2,5-dicyanobenzene (**6b**), 1,5-dicyano-2,6-dimethylnaphthalene, 9,10-bis(*p*-cyanophenyl)-2,6-bis(bromomethyl)anthracene (**9**) were prepared by the literature methods.^[5b,8a,8b,8e,13] Synthesis of other compounds is described below.

Compound 1a: A mixture of **5a** (0.47 g, 1.6 mmol), 4-(diethylamino)salicylaldehyde (0.63 g, 3.3 mmol), K_2CO_3 (1.4 g, 9.8 mmol), and Bu_4NHSO_4 (0.17 g, 0.49 mmol) was stirred in DMF (30 mL) for 8 h at 125 °C. The dark reaction mixture was diluted with water and extracted with ethyl acetate. The organic solvent was evaporated and the product was purified on a silica gel column by using hexane/ethyl acetate 3:1. The product was recrystallized from ethyl acetate/methanol to obtain yellow solid (0.34 g, 42%). M.p. 143 °C; ^1H NMR (300 MHz, CDCl_3): $\delta = 8.08$ (s, 1H), 8.02 (d, $J = 9.0$ Hz, 1H), 7.93 (d, $J = 9.0$ Hz, 1H), 7.62 (s, 1H), 7.42 (d, $J = 9.0$ Hz, 1H), 7.38 (d, $J = 9.0$ Hz, 1H), 6.97 (s, 1H), 6.80 (s, 1H), 6.78 (s, 1H), 6.71 (d, $J = 9.0$ Hz, 1H), 6.69 (d, $J = 9.0$ Hz, 1H), 3.43 (q, $J = 7.0$ Hz, 8H), 1.22 ppm (t, $J = 7.5$ Hz, 12H); IR (KBr): $\tilde{\nu} = 2220$ cm^{-1} (CN); elemental analysis calcd (%) for $\text{C}_{31}\text{H}_{31}\text{N}_3\text{O}_2$: C 77.96, H 6.54, N 8.80; found: C 77.89, H 6.60, N 8.82.

Compound 1b: Synthesized by the same procedure as described for **1a** except that **5b** was used. Recrystallization from ethyl acetate/petroleum ether gave black-red solid (48%). M.p. > 300 °C; ^1H NMR (300 MHz, CDCl_3): $\delta = 8.29$ (s, 2H), 7.69 (s, 2H), 7.43 (d, $J = 9.0$ Hz, 2H), 6.76 (s, 2H), 6.71 (d, $J = 9.0$ Hz, 2H), 3.43 (q, $J = 7.0$ Hz, 8H), 1.23 ppm (t, $J = 7.5$ Hz, 12H); IR (KBr): $\tilde{\nu} = 2221$ cm^{-1} (CN); elemental analysis calcd (%) for $\text{C}_{32}\text{H}_{30}\text{N}_4\text{O}_2$: C 76.47, H 6.02, N 11.15; found: C 76.35, H 6.17, N 11.10.

2-Cyano-1,4-bis[(2'-nitro-4'-dihexylamino)styryl]benzene (7a): NaOtBu (1.6 g, 16 mmol) was added to a solution containing **6a** (3.0 g, 7.4 mmol) in THF (80 mL) at 0 °C under N_2 . To this solution, 4-dihexylamino-2-ni-

trobenzaldehyde (5.0 g, 15 mmol) was added and the solution was stirred for 12 h at RT. Water was added to stop the reaction and the product was extracted with ethyl acetate and washed with brine. The organic layer was dried with MgSO_4 and the solvent was removed in vacuo to obtain the product (4.8 g, 84%). M.p. 110°C; $^1\text{H NMR}$ (300 MHz, CDCl_3): δ = 7.77 (d, J = 9.0 Hz, 1H), 7.69 (d, J = 9.0 Hz, 1H), 7.68 (s, 1H), 7.64 (d, J = 9.0 Hz, 1H), 7.57 (d, J = 9.0 Hz, 1H), 7.52 (d, J = 18.0 Hz, 1H), 7.32 (d, J = 18.0 Hz, 1H), 7.27 (d, J = 18.0 Hz, 1H), 7.11 (s, 1H), 7.10 (s, 1H), 6.85 (d, J = 9.0 Hz, 1H), 6.84 (d, J = 18.0 Hz, 1H), 6.81 (d, J = 9.0 Hz, 1H), 3.31 (t, J = 7.0 Hz, 8H), 1.60 (m, J = 7.0 Hz, 8H), 1.35 (m, 24H), 0.91 ppm (t, J = 7.5 Hz, 12H); IR (KBr): $\tilde{\nu}$ = 2223 cm^{-1} (CN); elemental analysis calcd (%) for $\text{C}_{47}\text{H}_{65}\text{N}_5$: C 73.88, H 8.57, N 9.17; found: C 73.68, H 8.91, N 9.20.

Compound 2a: A solution of **7a** (0.70 g, 0.92 mmol) in $\text{P}(\text{OEt})_3$ (10 mL) was heated under reflux overnight under N_2 . The solvent was removed in vacuo and the product was purified on a silica gel column by using hexane/ethyl acetate 8:1 to yield the title compound (0.24 g, 37%). M.p. 42°C; $^1\text{H NMR}$ (300 MHz, CDCl_3): δ = 8.66 (s, 1H), 8.09 (s, 1H), 7.82 (s, 1H), 7.73 (s, 2H), 7.46 (d, J = 9.0 Hz, 1H), 7.44 (d, J = 9.0 Hz, 1H), 7.04 (s, 1H), 6.76 (s, 1H), 6.66 (m, 4H), 3.31 (t, J = 7.0 Hz, 8H), 1.62 (m, J = 7.0 Hz, 8H), 1.33 (m, 24H), 0.90 ppm (t, J = 7.5 Hz, 12H); IR (KBr): $\tilde{\nu}$ = 2222 cm^{-1} (CN); elemental analysis calcd (%) for $\text{C}_{47}\text{H}_{65}\text{N}_5$: C 80.64, H 9.36, N 10.00; found: C 80.38, H 9.41, N 10.02.

2,5-Dicyano-1,4-bis[(2-nitro-4'-diethylamino)styryl]benzene (7b): Synthesized by the same procedure as described for **7a** except that **6b** was used. The product was purified by recrystallization from MeOH to yield the title compound (78%). M.p. 243°C; $^1\text{H NMR}$ (300 MHz, CDCl_3): δ = 8.01 (s, 2H), 7.69 (d, J = 18.0 Hz, 2H), 7.67 (d, J = 9.0 Hz, 2H), 7.19 (d, J = 18.0 Hz, 2H), 7.13 (s, 2H), 6.84 (d, J = 9.0 Hz, 2H), 3.34 (t, J = 7.5 Hz, 8H), 1.60 (m, 8H), 1.35 (m, 24H), 0.91 ppm (t, J = 7.5 Hz, 12H); IR (KBr): $\tilde{\nu}$ = 2223 cm^{-1} (CN); elemental analysis calcd (%) for $\text{C}_{48}\text{H}_{64}\text{N}_6$: C 73.06, H 8.18, N 10.65; found: C 73.09, H 8.31, N 10.56.

Compound 2b: Synthesized by the same procedure as described for **2a** except that **7b** was used to yield the title compound (24%). M.p. 208°C; $^1\text{H NMR}$ (300 MHz, CDCl_3): δ = 8.57 (s, 2H), 7.95 (s, 2H), 7.45 (d, J = 9.0 Hz, 2H), 7.08 (s, 2H), 6.68 (d, J = 9.0 Hz, 2H), 6.55 (s, 2H), 3.34 (t, J = 7.0 Hz, 8H), 1.60 (m, J = 7.0 Hz, 8H), 1.35 (m, 24H), 0.91 ppm (t, J = 7.5 Hz, 12H); IR (KBr): $\tilde{\nu}$ = 2223 cm^{-1} (CN); elemental analysis calcd (%) for $\text{C}_{48}\text{H}_{64}\text{N}_6$: C 79.51, H 8.90, N 11.59; found: C 79.30, H 8.98, N 11.65.

2,6-Bis(bromomethyl)-1,5-dicyanophthalene (8): NBS (30 g, 0.17 mol) and benzoyl peroxide (0.40 g, 1.7 mmol) were added to a solution containing 1,5-dicyano-2,6-dimethylnaphthalene (10 g, 76 mmol) in benzene (300 mL). The mixture was vigorously stirred under reflux for 2 h. After usual work-up, the product was purified on a silica gel column by using hexane/methylene chloride 1:1. The product was recrystallized from chloroform to obtain white crystals (13 g, 61%). M.p. 257°C; $^1\text{H NMR}$ (300 MHz, CDCl_3): δ = 8.47 (d, J = 9.0 Hz, 2H), 7.86 (d, J = 9.0 Hz, 2H), 4.84 ppm (s, 4H); elemental analysis calcd (%) for $\text{C}_{16}\text{H}_{10}\text{N}_4\text{O}_2$: C 46.19, H 2.22, N 7.70; found: C 46.22, H 2.21, N 7.73.

Compound 3b: Synthesized by the same procedure as described for **1a** except that **8** was used to yield the title compound (45%). M.p. > 300°C; $^1\text{H NMR}$ (300 MHz, CDCl_3): δ = 8.48 (d, J = 9.0 Hz, 2H), 8.27 (d, J = 9.0 Hz, 2H), 7.82 (s, 2H), 7.48 (d, J = 9.0 Hz, 2H), 6.81 (s, 2H), 6.75 (d, J = 9.0 Hz, 2H), 3.46 (q, J = 7.0 Hz, 8H), 1.24 ppm (t, J = 7.5 Hz, 12H); IR (KBr): $\tilde{\nu}$ = 2223 cm^{-1} (CN); elemental analysis calcd (%) for $\text{C}_{36}\text{H}_{32}\text{N}_4\text{O}_2$: C 78.24, H 5.84, N 10.14; found: C 78.31, H 5.79, N 10.20.

Compound 4b: Synthesized by the same procedure as described for **1a** except that **9** was used to yield the title compound (34%). M.p. > 300°C; $^1\text{H NMR}$ (300 MHz, CDCl_3): δ = 8.01 (d, J = 9.0 Hz, 4H), 7.87 (s, 2H), 7.72 (d, J = 9.0 Hz, 2H), 7.69 (d, J = 9.0 Hz, 4H), 7.51 (d, J = 9.0 Hz, 2H), 7.35 (d, J = 9.0 Hz, 2H), 6.92 (s, 2H), 6.74 (s, 2H), 6.68 (d, J = 9.0 Hz, 2H), 3.42 (q, J = 7.0 Hz, 8H), 1.21 ppm (t, J = 7.5 Hz, 12H); IR (KBr): $\tilde{\nu}$ = 2220 cm^{-1} (CN); elemental analysis calcd (%) for $\text{C}_{32}\text{H}_{42}\text{N}_4\text{O}_2$: C 82.73, H 5.61, N 7.42; found: C 82.85, H 5.70, N 7.56.

Vesicle preparation: To prepare small GUVs, we followed the solvent evaporation method developed by Moscho et al.^[10a] To a 50 mL round-bottomed flask containing CHCl_3 (1 mL), 1,2-dipalmitoyl-*sn*-glycero-3-

phosphocholine (DPPC) phospholipid in CHCl_3 (5 mg mL^{-1} , 6.8×10^{-3} M, 30 μL) and **1-3** (1.0×10^{-3} M, 2.0 μL) were added (lipid/fluorophore 100:1). The Millipore water (5.0 mL) was then carefully added along the flask walls. The chloroform was removed in a rotary evaporator (Buechi R-114) under reduced pressure at 45°C (Buechi waterbath B-480) for 2 min. The mean diameter of vesicles was $\sim 10 \mu\text{m}$ (Figure S2a).

To grow large GUVs, the electroformation method was employed.^[10b,c] The chamber for the GUVs preparation consisted of two ITO-coated glasses separated by a silicon spacer (thickness = 0.5 mm). DPPC was dissolved in CHCl_3 at a concentration of 0.3 mg mL^{-1} . 3 μL of this solution were deposited on one of the conductive coated glasses and dried using a nitrogen stream. Previously heated (50°C) Millipore water was added and then an AC field of 10 Hz, 1 V was applied by using a function generator (Stanford Research System, DS345) at 50°C (Aldrich Airbath oven) for 3 h. After the vesicle was produced, a small amount (< 2 μL) of fluorophore in DMSO was added. The mean diameter of vesicles was $\sim 100 \mu\text{m}$. Large GUVs with a mean diameter of $\sim 200 \mu\text{m}$ were used for the photostability test (Figure S2b).

Spectroscopic measurements: Absorption spectra were recorded on a Hewlett-Packard 8453 diode array spectrophotometer, and the fluorescence spectra were obtained with a Amico Bowman series 2 luminescence spectrometer. The fluorescence quantum yield was determined by using fluorescein and rhodamine B as the reference.^[14] Fluorescence lifetimes were measured using the time-correlated single photon counting (TCSPC) method with a femto second laser system (Verdi/Mira 900, Coherent Radiation, Palo Alto, CA) as described.^[15] Molar absorptivity and emission spectra for **1-4** in toluene are depicted in Figure 1.

The fluorescence spectra and fluorescence lifetimes of the GUVs were measured using the GUVs in the buffer solution (pH 7.0). The fluorescence spectra of the GUVs are shown in Figure S1.

Measurement of two-photon cross-sections: The experimental setup for the two-photon fluorescence (TPF) measurement is described elsewhere.^[3] The two-photon cross-section δ was calculated by using the two-photon-induced fluorescence measurement technique with the following Equation:

$$\delta = \frac{S_s \Phi_r \phi_r c_r}{S_r \Phi_s \phi_s c_s} \delta_r$$

in which the subscripts *s* and *r* refer to the sample and reference molecules.^[8a] The intensity of the signal collected by a CCD detector was denoted as *S*. Φ is the fluorescence quantum yield. ϕ is the overall fluorescence collection efficiency of the experimental apparatus. The number density of the molecules in solution was denoted as *c*. δ_r is the TPA cross-section of the reference molecule. Samples were dissolved in toluene at concentrations of 5.0×10^{-6} M and the two-photon induced fluorescence intensity was measured at 740–1050 nm by using fluorescein (8.0×10^{-6} M, pH 11) and rhodamine B (1×10^{-5} M in MeOH) as the reference; the two-photon properties of the latter have been well characterized in the literature.^[16]

Photostability test: Photostability was determined with a DM IRE2 Microscope (Leica) excited by a mode-locked titanium/sapphire laser (Verdi/Mira 900, coherent radiation, Palo Alto, CA). To determine the rates of decrease of the two-photon excited fluorescence (TPEF) intensity of the dyes in GUVs, the digitized intensity (8 bit) from the GUV images was recorded for 1 s with 1.5 s intervals for the duration of one hour using *xyt* mode (λ = 800 nm, ~ 180 fs, I = 1–3 $\text{mW } \mu\text{m}^{-2}$). The TPEF of large and small GUVs were collected by using $\times 10$ objective lens (NA = 0.30 DRY) and $\times 100$ objective lens (NA = 1.30 OIL), respectively. The laser power used for the small GUVs was estimated to be $\sim 110 \text{ mW } \mu\text{m}^{-2}$. In all cases, the TPEF intensity showed 1st order decay with time. The plots of $\ln(I - I_\infty)/(I_0 - I_\infty)$ versus irradiation time for the small GUVs labeled with **1-3** are shown in Figure S3. The slopes of these plots are the 1st order decay constants. Half-lives ($t_{1/2}$) were calculated by using the relationship, $t_{1/2} = 0.693/k$.

Acknowledgements

We acknowledge financial support from KOSEF (R02-2004-000-10006-0) and CRM-KOSEF. H.M.K. was supported by the BK21 program.

- [1] a) M. D. Cahalan, I. Parker, S. H. Wei, M. J. Miller, *Nat. Rev. Immunol.* **2002**, 2, 872–880; b) W. R. Zipfel, R. M. Williams, W. W. Webb, *Nat. Biotechnol.* **2003**, 21, 1369–1377.
- [2] P. T. C. So, C. Y. Dong, B. R. Masters, K. M. Berland, *Annu. Rev. Biomed. Eng.* **2000**, 2, 399–429.
- [3] S. K. Lee, W. J. Yang, J. J. Choi, C. H. Kim, S.-J. Jeon, B. R. Cho, *Org. Lett.* **2005**, 7, 323–326.
- [4] H. Y. Woo, J. W. Hong, B. Liu, A. Mikhailovsky, D. Korystov, G. C. Bazan, *J. Am. Chem. Soc.* **2005**, 127, 820–821.
- [5] a) J. K. J. Pond, O. Tsutsumi, M. Rumi, O. Kwon, E. Zojer, J.-L. Brédas, S. R. Marder, J. W. Perry, *J. Am. Chem. Soc.* **2004**, 126, 9291–9306; b) H. M. Kim, M.-Y. Jeong, H. C. Ahn, S.-J. Jeon, B. R. Cho, *J. Org. Chem.* **2004**, 69, 5749–5751.
- [6] M. H. W. Werts, S. Gmouh, O. Mongin, T. Pons, M. Blanchard-Desce, *J. Am. Chem. Soc.* **2004**, 126, 16294–16295.
- [7] a) K. D. Belfield, M. V. Bondar, O. V. Przhonska, K. J. Schafer, *J. Photochem. Photobiol. A* **2004**, 162, 489–496; b) K. D. Belfield, M. V. Bondar, O. V. Przhonska, K. J. Schafer, *Photochem. Photobiol. Sci.* **2004**, 3, 138–141; c) O. Mongin, L. Porrès, L. Moreaux, J. Mertz, M. Blanchard-Desce, *Org. Lett.* **2002**, 4, 719–722; d) L. Porrès, O. Mongin, C. Katan, M. Charlot, T. Pons, J. Mertz, M. Blanchard-Desce, *Org. Lett.* **2004**, 6, 47–50.
- [8] a) S. J. K. Pond, M. Rumi, M. D. Levin, T. C. Parker, D. Beljonne, M. W. Day, J.-L. Brédas, S. R. Marder, J. W. Perry, *J. Phys. Chem. A* **2002**, 106, 11470–11480; b) B. Strehmel, A. M. Sarker, H. Detert, *ChemPhysChem* **2003**, 4, 249–259; c) O.-K. Kim, K.-S. Lee, H. Y. Woo, K.-S. Kim, G. S. He, J. Swiatkiewicz, P. N. Prasad, *Chem. Mater.* **2000**, 12, 284–286; d) L. Ventelon, S. Charier, L. Moreaux, J. Mertz, M. Blanchard-Desce, *Angew. Chem.* **2001**, 113, 2156–2159; *Angew. Chem. Int. Ed.* **2001**, 40, 2098–2101; e) W. J. Yang, D. Y. Kim, M.-Y. Jeong, H. M. Kim, S.-J. Jeon, B. R. Cho, *Chem. Commun.* **2003**, 2618–2619.
- [9] G. Grynkiewicz, M. Poenie, R. Y. Tsien, *J. Biol. Chem.* **1985**, 260, 3440–3450.
- [10] a) A. Moscho, O. Orwar, D. T. Chiu, B. P. Modi, R. N. Zare, *Proc. Natl. Acad. Sci. USA* **1996**, 93, 11443–11447; b) M. I. Angelova, D. S. Dimitrov, *Faraday Discuss. Chem. Soc.* **1986**, 81, 303–311; c) M. I. Angelova, S. Soleau, P. Meleard, J. F. Faucon, P. Bothorel, *Prog. Colloid Polym. Sci.* **1992**, 89, 127–131.
- [11] L. A. Bagatolli, E. Gratton, *Biophys. J.* **1999**, 77, 2090–2101.
- [12] a) H. Giloh, J. W. Sedat, *Science* **1982**, 217, 1252–1255; b) D. M. Benson, J. Bryan, A. L. Plant, A. M. Gotto, Jr., L. C. Smith, *J. Cell Biol.* **1985**, 100, 1309–1323.
- [13] V. Vesely, F. Stursa, *Collect. Czech. Chem. Commun.* **1932**, 4, 21–31.
- [14] J. N. Demas, G. A. Crosby, *J. Phys. Chem.* **1971**, 75, 991–1024.
- [15] D. V. O'Connor, D. Phillips, *Time-correlated Single Photon Counting*, Academic Press, London, **1984**.
- [16] C. Xu, W. W. Webb, *J. Opt. Soc. Am. B* **1996**, 13, 481–491.

Received: March 25, 2005
Published online: August 5, 2005